Chinese Chemical Letters 35 (2024) 109499

Contents lists available at ScienceDirect

Chinese Chemical Letters

journal homepage: www.elsevier.com/locate/cclet

# Percarbonate activation catalyzed by nanoblocks of basic copper molybdate for antibiotics degradation: High performance, degradation pathways and mechanism

Xiaotao Jin[a], Yanlan Wang[b], Yingping Huang[a], Di Huang[a,*], Xiang Liu[a,*]

[a] Engineering Research Center of Eco-Environment in Three Gorges Reservoir Region of Ministry of Education, College of Materials and Chemical Engineering, China Three Gorges University, Yichang 443002, China

[b] Department of chemistry and chemical engineering, Liaocheng University, Liaocheng 252059, China

ARTICLE INFO

*Article history:*
Received 27 September 2023
Revised 13 December 2023
Accepted 2 January 2024
Available online 10 January 2024

*Keywords:*
Sodium percarbonate
Fenton process
Water treatment
Copper molybdate
Nanoblocks

ABSTRACT

Sodium percarbonate ($Na_2CO_3·1.5H_2O_2$, SPC) has been extensively employed as a solid substitute of $H_2O_2$ for Fenton process in water treatment, because of its high stability during the production, transport, storage and usage. In addition, SPC can be applied in a wider range of work pH, it is also applied as a buffer in Fenton reaction for preventing a drop in pH. Herein, we have synthesized basic copper molybdate (BCM) nanoblocks with the molecular formula of $Cu_3(MoO_4)_2(OH)_2$ as an efficient and heterogeneous catalyst for antibiotics degradation *via* percarbonate activation. First, fully physical characterizations confirmed BCM nanocomposite exhibited a structure of nanoblocks. We also found that BCM/SPC system could work in a much wider pH range, compared with $H_2O_2$. Then, BCM/SPC system presented a good anti-interference ability for natural organic matter in OTC degradation. EPR results and Quenching tests confirmed that the co-presence of $^{\cdot}CO_3^-$, $^{\cdot}O_2^-$, $^1O_2$ and $^{\cdot}OH$ in BCM/SPC system.



Currently, medicine residues (peculiarly antibiotics) has aroused wide concern because of their omnipresent emergence and potential harmful impact on the water eco-environment [1–4]. The predictability of future results show the world consumption of antibiotics will grow rapidly to 110,000 tons in 2030 [5–9]. These abused antibiotics are widely found in a variety of water environment, including rivers, lakes, groundwater and effluent from sewage treatment plant, even our drinking water [10–16]. Among antibiotics, oxytetracycline (OTC), a type of tetracycline antibiotics, is comprehensively applied for veterinary and human medicine [17–24]. In fact, the OTC concentration in groundwater and surface water was detected to be ng/L to μg/L level, which could pose a significant threat to the public health and ecosystem even at trace concentration [25–27]. As a result, it is of high importance to exploit the efficient and green methods for achieving effective antibiotics removal [28–32].

The Fenton process *via* $H_2O_2$ activation is deemed as the most promising process for degrading antibiotics by reason of its high-efficiency [33–37]. However, its full-scale and practical application was restricted by some unavoidable detriments, such as the high transportation cost and explosibility of $H_2O_2$, iron sludge problem and narrow pH ranges (2.5–3.0) of Fenton process [38–41]. Recent, sodium percarbonate ($Na_2CO_3·1.5H_2O_2$, SPC) has been extensively employed as a solid substitute of $H_2O_2$ for Fenton process in water treatment, because of its high stability during the production, transport, storage and usage [42–48]. In addition, SPC can be applied in a wider range of work pH, it is also applied as a buffer in Fenton reaction for preventing a drop in pH [49–53]. As part of our group's current interest on the sewage remediation [54], herein, we have first synthesized basic copper molybdate (BCM) nanoblocks with the molecular formula of $Cu_3(MoO_4)_2(OH)_2$ as an efficient and heterogeneous catalyst for antibiotics degradation *via* percarbonate activation. First, the structure and morphology of BCM nanoblocks was investigated by fully physical characterizations. Then, the performance, degradation pathways and mechanism of OTC degradation catalyzed by BCM nanoblocks *via* percarbonate activation were investigated.

As demonstrated in Fig. S1 (Supporting information), BCM nanoblocks was synthesized by hydrothermal reaction of $Na_2MoO_4$ and $Cu(NO_3)_2·xH_2O$ at 150 °C for 6 h. The nature crystalline phase of BCM nanoblocks was evaluated by XRD. The characteristic diffraction peaks of $Cu_3(MoO_4)_2(OH)_2$ (020), (021), ($\bar{1}$01), (130) and (200) lattice planes clearly appeared in Fig. S2a (Sup-

* Corresponding authors.
*E-mail addresses:* huangd94@iccas.ac.cn (D. Huang), xiang.liu@ctgu.edu.cn (X. Liu).

https://doi.org/10.1016/j.cclet.2024.109499
1001-8417/

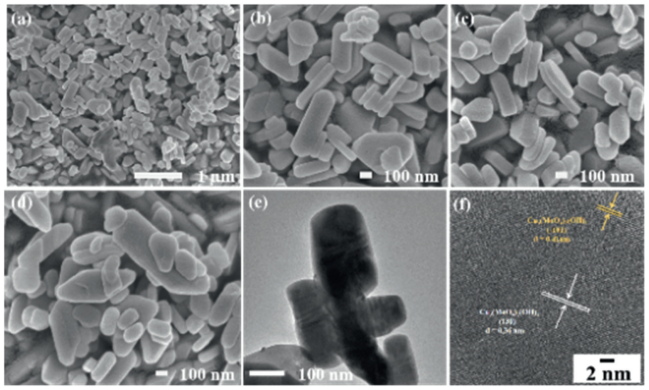


**Fig. 1.** (a-d) SEM, (e) TEM and (f) HRTEM of BCM nanoblocks.

porting information), illustrating the synthesis of $Cu_3(MoO_4)_2(OH)_2$ [55]. In Fig. S2b (Supporting information), texture structure of BCM nanoblocks was checked by BET. BCM nanoblocks exhibited a mean pore diameter of 0.697 nm, total pore volume of 0.048 $cm^3/g$ and BET surface area of 6.683 $m^2/g$, suggesting a micropore structure [56]. As shown in Fig. S2c (Supporting information), the sum XPS of BCM nanoblocks exhibited that the co-existence of Cu, Mo and O. The pair peaks of 934.70 eV and 954.53 eV appeared in Fig. S2d (Supporting information), illustrating the presence of Cu(II) [57]. In Fig. S2e (Supporting information), the Mo 3d was divided into two peaks of 232.31 eV (Mo $3d_{5/2}$) and 235.45 eV (Mo $3d_{3/2}$), which was assigned to $Mo^{VI}$ [58–60]. As presented in Fig. S2f (Supporting information), the O 1s was divided into two peaks of lattice oxygen ($O_{latt}$, 530.36 eV) and adsorbed oxygen ($O_{ads}$, 531.56 eV) [55]. Furthermore, the morphology and nanostructure of BCM nanoblocks was also determined by scanning electron microscope (SEM), transmission electron microscope (TEM), and high resolution TEM (HRTEM). As shown in Figs. 1a-e, BCM nanocomposite exhibited a structure of nanoblocks. As demonstrated in Fig. 1f, $Cu_3(MoO_4)_2(OH)_2$ ($\bar{1}01$) and (130), whose lattice distances were 0.41 nm *resp.* 0.36 nm, were recorded in BCM nanoblocks, further confirming the formation of $Cu_3(MoO_4)_2(OH)_2$ [61]. In addition, the precise localization of Cu, Mo and O elements in BCM nanoblocks was also measured by EDX elements mapping. In Figs. 2a-e and Fig. S3 (Supporting information), it is clear that BCM nanoblocks was composed of Cu, Mo and O elements, suggesting the formation of $Cu_3(MoO_4)_2(OH)_2$.

For studying the catalytic activity of BCM nanoblocks in OTC degradation by percarbonate activation, OTC degradation over $Fe_2(MoO_4)_3$, $NiMoO_4$ and BCM nanoblocks were tested in Fig. S4 (Supporting information). First, $NiMoO_4$ and $Fe_2(MoO_4)_3$ were

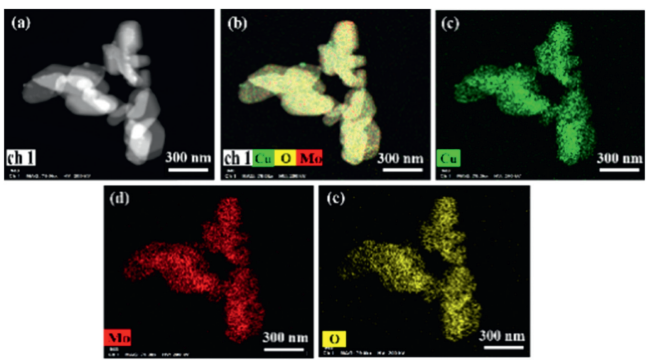


**Fig. 2.** (a) STEM, (b) combined Cu, Mo and O, (c) Cu, (d) Mo, (e) O compositional mapping.

synthesized under the same process as BCM nanoblocks. Then, $Fe_2(MoO_4)_3$ and $NiMoO_4$ were measured by XRD and SEM. Figs. S5 and S6 (Supporting information) exhibited that the successful formation of $Fe_2(MoO_4)_3$ and $NiMoO_4$ in XRD. The SEM result exhibited that $Fe_2(MoO_4)_3$ and $NiMoO_4$ possessed a nanoblock (Fig. S7 in Supporting information) and nanorod (Fig. S8 in Supporting information) structure, respectively. The OTC degradation was conducted by 20 mg/L of OTC, 0.2 g/L of sodium percarbonate, 0.25 g/L of catalyst and 50 mL of deionized water at 30 °C. The order of OTC degradation efficiency as follow: BCM nanoblocks (80.01%) > $Fe_2(MoO_4)_3$ (59.99%) > $NiMoO_4$ (12.12%), highlighting the key role of BCM nanoblocks in activating SPC to degrade OTC.

As BCM nanoblocks presented the superior catalytic activity in OTC degradation, its kinetic study, including BCM nanoblocks concentration, SPC concentration, initial OTC concentration and degradation temperature, had been further investigated. First, OTC degradation was carried out with various BCM nanoblocks concentrations from 0.1 g/L to 0.49 g/L. Fig. 3a elucidated that OTC degradation rate was positive correlation, where the slope is 0.3, with BCM nanoblocks concentrations. Next, the impression of SPC concentration on OTC degradation was also tested in Fig. 3b, OTC removal efficiency was heightened, with slope of 0.27, as the increase of SPC concentration. Then, OTC degradation was carried out with different initial OTC concentrations from 10 mg/L to 50 mg/L. Fig. 3c illustrated that OTC removal efficiency decreased with the increase of initial OTC concentrations. In Fig. 3d, it is clear that OTC degradation efficiency rose as the enhancement of degradation temperature. Based on the Arrhenius law, the $E_a$ was found to be 55.79 kJ/mol, Moreover, tetracycline (TC) and chlorotetracycline (CTC) had been also degraded by BCM/SPC system in 40 min (Fig. S9 in Supporting information).

The stability of BCM nanoblocks in OTC degradation *via* percarbonate activization was also tested for further practical application [62]. When OTC degradation was over, BCM nanoblocks was re-obtained and recycled by filtration for the next degradation. As demonstrated in Fig. 3e, BCM nanoblocks had been successfully reused 5 times in OTC degradation without any efficiency decrease. Then, $5^{th}$ reused BCM nanoblocks was measured by XRD and SEM, the result exhibited that $5^{th}$ reused BCM nanoblocks remained the same crystalline state (Fig. S10 in Supporting information) and morphology (Fig. S11 in Supporting information) as the fresh one. In addition, the Cu concentration in the solution, after completion of OTC degradation, was less than 1 ppm upon by ICP, confirming BCM was a true heterogeneous catalyst on OTC degradation.

As pH played a key parameter on the OTC degradation, OTC removal over BCM/SPC system was further conducted at various initial pH from 3 to 11. Fig. 3f described that BCM/SPC system played the highly catalytic performance in OTC removal at pH 3-11. This result confirmed that BCM/SPC system could work in a much wider pH range, compared with $H_2O_2$ [63]. The effect of humic acids (HA), as the common natural organic matter, on OTC degradation catalyzed by BCM/SPC system was also measured in Fig. 3g [64]. It is clear that HA played a negligible role on OTC degradation, even at 50 mg/L of HA, indicating that the BCM/SPC system owned an excellent anti-interference ability for natural organic matter in OTC degradation.

For revealing the mechanism of OTC degradation *via* percarbonate activation, the reactive oxygen species (ROS) in BCM/SPC system had been identified by quenching experiments. Explicitly PhOH, benzoquinone (BQ), $NaN_3$ and EtOH were used for quenching $^{\cdot}CO_3^-$, $^{\cdot}O_2^-$, $^1O_2$ and $^{\cdot}OH$, respectively [65]. As presented in Fig. 3h, it is clear that all of PhOH (3.98 mmol/L), BQ (0.2 mmol/L), $NaN_3$ (0.2 mmol/L) and EtOH (1.6 mol/L) exhibited an inhibitory effect on OTC degradation. This result indicated the co-presence of $^{\cdot}CO_3^-$, $^{\cdot}O_2^-$, $^1O_2$ and $^{\cdot}OH$ in BCM/SPC system, which was also con-

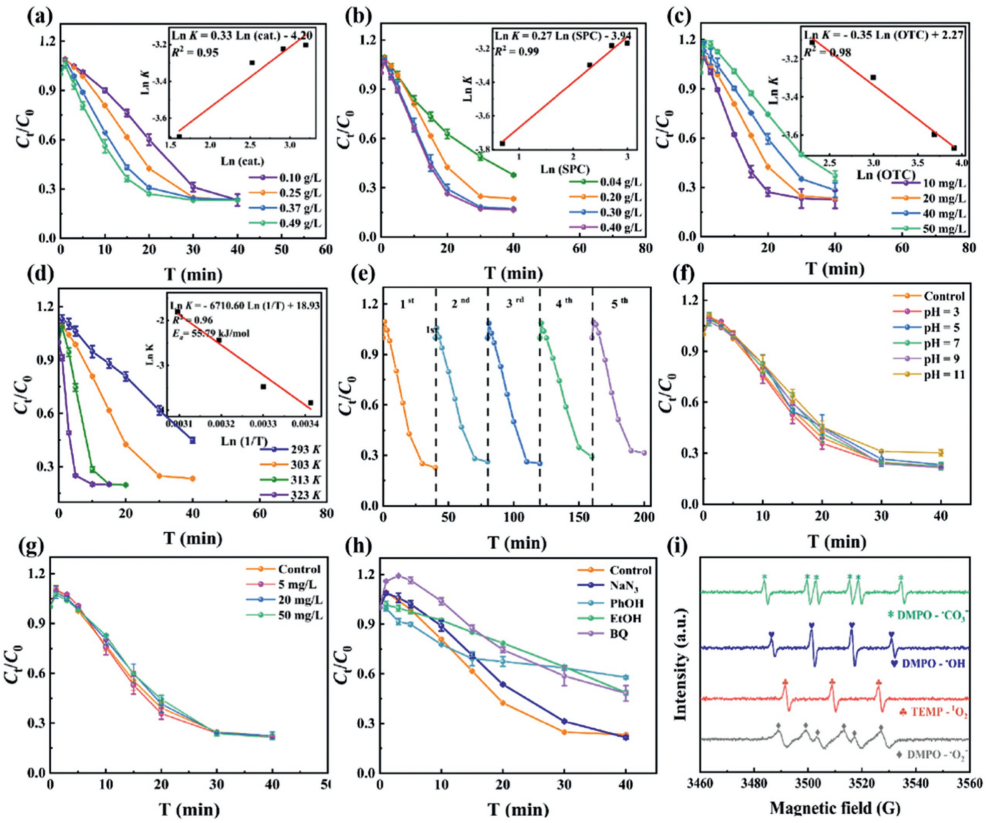


**Fig. 3.** Influences of (a) BCM nanoblocks, (b) SPC concentration, (c) initial OTC concentration, (d) degradation temperature, (e) stability of BCM nanoblocks, (f) pH, (g) humic acid on OTC degradation. (h) Effect of BQ (0.2 mmol/L), $NaN_3$ (0.2 mmol/L), EtOH (1.6 mol/L) and PhOH (3.98 mmol/L) on OTC degradation over BCM/SPC. (i) EPR spectra of BCM/SPC system. Reaction Condition: 20 mg/L of OTC, 0.25 g/L of BCM, 0.2 g/L of SPC at 30 °C.

firmed by EPR analysis (Fig. 3i). Then, the dosage of PhOH, BQ, $NaN_3$, or EtOH was reduced to 0.2 mmol/L. As shown in Fig. S12 (Supporting information), the result indicated that only BQ played a inhibitory effect on OTC degradation, suggesting $^{\cdot}O_2^-$ was the major ROS in BCM/SPC system. For investigating the possible OTC degradation pathways, the total content of organic carbon (TOC) and high resolution mass spectrum (HR-MS) were employed to measure the degraded OTC solution for determining its mineralization rate and degradation intermediates. The TOC analysis indicated 15.62% of OTC were completely mineralized into $CO_2$ and $H_2O$. As it can been seen in Fig. S13 (Supporting information), OTC molecule peak of *m/z* 461 disappeared in HR-MS, suggesting that OTC molecules were degraded into small intermediates. In Fig. S14 (Supporting information), fourteen kinds of intermediates had been confirmed by Mass library [66,67]. Based on quenching tests, EPR result, HR-MS analysis and relevant literature [68,69], a plausible mechanism of OTC degradation over BCM/SPC system was proposed in Fig. 4. First, OTC and SPC molecules wereanchored at the surface of BCM nanoblocks. Immediately, SPC molecules were decomposed into $^{\cdot}CO_3^-$, $^{\cdot}O_2^-$, $^1O_2$ and $^{\cdot}OH$ by BCM nanoblocks. Then, OTC molecules, after the attack of multiple reactive oxygen species, were degraded into short-chain intermediates, which were further mineralized into $CO_2$ and $H_2O$.

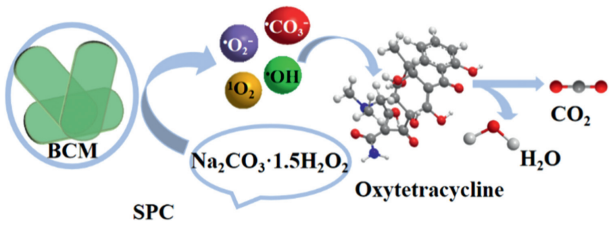


**Fig. 4.** Mechanism of SPC activation and OTC degradation on BCM.

In addition, this BCM/SPC system's catalytic performance with other catalytic systems for OTC degradation was also compared in Table S1 (Supporting information) [66,70–76]. The result shown that BCM exhibited the superior catalytic performance in activating SPC for OTC degradation.

In summary, basic copper molybdate (BCM) nanoblock with the molecular formula of $Cu_3(MoO_4)_2(OH)_2$ has been synthesized as an efficient and heterogeneous catalyst for antibiotics degradation *via* percarbonate activation. First, fully physical characterizations confirmed BCM nanocomposite exhibited a structure of nanoblocks. Compared with other molybdates, the order of OTC degradation efficiency as follow: BCM nanoblocks (80.01%)> $Fe_2(MoO_4)_3$ (59.99%) > $NiMoO_4$ (12.12%), highlighting the key role of BCM nanoblocks in activating SPC to degrade OTC. We also found that BCM/SPC system could work in a much wider pH range, compared with $H_2O_2$. Then, BCM/SPC presented a high anti-interference ability for natural organic matter in OTC removal. EPR results and Quenching tests demonstrated that the co-presence of $^{\cdot}CO_3^-$, $^{\cdot}O_2^-$, $^1O_2$ and $^{\cdot}OH$ in BCM/SPC system. This study provides an excellent Mo-based catalyst for activating percarbonate in antibiotics removal.

## Declaration of competing interest

The authors declare that they have no known competing financial interests or personal relationships that could have appeared to influence the work reported in this paper.

## Acknowledgments

Financial support from the NSFC (Nos. 21972073, 22136003, 21805166 and 22206188), the 111 Project of China (No. D20015)

and Natural Science Foundation of Hubei Province, China (No. 2022CFB275) is gratefully acknowledged, and the authors thank eceshi (www.eceshi.com) for TEM analysis.

## Supplementary materials

Supplementary material associated with this article can be found, in the online version, at doi:10.1016/j.cclet.2024.109499.

## References

[1] Y. Li, H. Dong, L. Li, et al., Water Res. 202 (2021) 117451.
[2] R. Tian, H. Dong, J. Chen, R. Li, Q. Xie, Sep. Purif. Technol. 250 (2020) 117246.
[3] S. Singla, S. Sharma, S. Basu, N.P. Shetti, T.M. Aminabhavi, Int. J. Hydrogen Energy 46 (2021) 33696–33717.
[4] R. Koutavarapu, C.V. Reddy, K. Syed, et al., Chemosphere 267 (2021) 128559.
[5] T. Van-Boeckel, C. Brower, M. Gilbert, et al., Proc. Natl. Acad. Sci. U. S. A. 112 (2015) 5649–5654.
[6] B. Wang, B. Ni, Z. Yuan, J. Guo, Water Res. 173 (2020) 115592.
[7] H. Zhang, C. Zhou, H. Zeng, L. Deng, Z. Shi, J. Hazard. Mater. 395 (2020) 122613.
[8] C. Du, Z. Zhang, G. Yu, et al., Chemosphere 272 (2021) 129501.
[9] M. Srinivas, R.C. Venkata, R.R. Kakarla, et al., Res. Express. 6 (2019) 125502.
[10] L. Jia, R. Chen, J. Xu, et al., J. Hazard. Mater. 413 (2021) 125296.
[11] Y. Shao, Y. Wang, Y. Yuan, Y. Xie, Sci. Total Environ. 798 (2021) 149205.
[12] P. Tan, H. Fu, X. Ma, Nano Today 39 (2021) 101229.
[13] J. He, M. Shi, Y. Liang, B. Guo, Chem. Eng. J. 394 (2020) 124888.
[14] Q. Li, J. Ruan, X. Zhang, et al., Chem. Eng. J. 479 (2024) 147555.
[15] Z. Hao, W. Hou, C. Fang, Y. Huang, X. Liu, J. Hazard. Mater. 439 (2022) 129618.
[16] R. Hassandoost, A. Kotb, Z. Movafagh, et al., Chem. Eng. J. 431 (2022) 133851.
[17] Q. Chen, S. Wu, Y.J. Xin, Chem. Eng. J. 302 (2016) 377–387.
[18] Y. Liu, X. He, X. Duan, Y. Fu, D. Dionysiou, Chem. Eng. J. 276 (2015) 113–121.
[19] W. Jo, S. Kumar, M. Isaacs, A. Lee, S. Karthikeyan, Appl. Catal. B: Environ. 201 (2017) 159–168.
[20] H. Zhang, J. Wang, B. Zhou, et al., Environ. Pollut. 243 (2018) 1550–1557.
[21] Y. Liu, X. He, Y. Fu, D. Dionysios, J. Hazard. Mater. 305 (2016) 229–239.
[22] Y. Yang, G. Zeng, D. Huang, C. Zhang, et al., Appl. Catal. B: Environ. 272 (2020) 118970.
[23] N. Lia, L. Zhou, X. Jin, G. Owens, Z. Chen, J. Hazard. Mater. 366 (2019) 563–572.
[24] H. Zhang, Y. Mei, F. Zhu, et al., Chemosphere 306 (2022) 135635 -135635.
[25] Y. Peng, M. Cui, Z. Zhang, et al., ACS Catal. 12 (2019) 10803–10811.
[26] J. Wang, R. Zhuan, Sci. Total Environ. 701 (2020) 135023.
[27] N. Shetti, S. Malode, R. Malladi, Microchem. J. 146 (2019) 387–392.
[28] F. Zhu, Q. Ji, Y. Lei, et al., Chemosphere 291 (2022) 132765.
[29] M. Moradi, B. Kakavandi, A. Bahadoran, et al., Sep. Purif. Technol. 285 (2022) 120313.
[30] J. Zhou, H. Cheng, J. Ma, et al., Sep. Purif. Technol. 261 (2021) 18290.
[31] F. Zhu, S. Zhou, M. Sun, et al., Chemosphere 286 (2022) 131647.
[32] M. Rani, U. Shanker, J. Environ. Chem. Eng. 8 (2020) 104040.
[33] L. Peng, Y. Shang, B. Gao, X. Xu, Appl. Catal. B: Environ. 282 (2021) 119484.
[34] Y. Shang, X. Xu, B. Gao, S. Wang, X. Duan, Chem. Soc. Rev. 50 (2021) 5281–5322.
[35] S. Wang, Y. Lin, B. Shao, et al., Environ. Sci. Technol. 57 (2023) 9332–9341.
[36] S. Wang, J. Qian, B. Zhang, et al., Environ. Sci. Technol. 57 (2023) 1907–1918.
[37] L. Li, J. Huang, X. Hu, et al., Chemosphere 215 (2019) 647–656.
[38] C. Hung, C. Huang, C. Chen, et al., Environ. Pollut. 265 (2020) 114914.
[39] T. Zhang, Y. Chen, T. Wang, et al., J. Hazard. Mater. 448 (2023) 130875.
[40] Y. Liu, Y. Xia, Y. Xiong, et al., Sep. Purif. Technol. 322 (2023) 124256.
[41] Z. Mo, Z. Tan, J. Liang, et al., Chem. Eng. J. 457 (2023) 141150.
[42] X. Xu, Y. Zhou, S. Li, et al., J. Environ. Chem. Eng. 10 (2022) 108702.
[43] M. Che, J. Xiao, C. Shan, et al., Water Res. 243 (2023) 120420.
[44] V.N. Rao, P. Ravi, M. Sathish, et al., J. Hazard. Mater. 415 (2021) 125588.
[45] K. Kyere-Yeboah, X. Qiao, Chemosphere 336 (2023) 139246.
[46] J. Liang, Z. Tan, L. Zhang, et al., Chem. Eng. J. 465 (2023) 142863.
[47] H. Xue, J. Li, G. Zhang, et al., Chemosphere 329 (2023) 138681.
[48] U. Farooq, F. Wang, J. Shang, et al., Chem. Eng. J. 454 (2023) 139996.
[49] H. Gao, H. Yu, Y. Jun, et al., Chemosphere 311 (2023) 137131.
[50] Z. Shangguan, X. Yuan, C. Qin, et al., Chem. Eng. J. 457 (2023) 141046.
[51] K. Fedorov, M. Rayaroth, N. Shah, G. Boczkaj, Chem. Eng. J. 456 (2023) 141027.
[52] X. Sheng, Y. Liu, R. Yang, et al., Sep. Purif. Technol. 326 (2023) 124772.
[53] C. Fang, Z. Hao, Y. Wang, et al., J. Clean. Prod. 405 (2023) 136912.
[54] V.N. Rao, V. Preethi, U. Bhargav, et al., Environ. Res. 199 (2021) 111323.
[55] J. Liao, Y. Wu, Y. Feng, et al., Catalysts 12 (2022) 426.
[56] X. Zhu, Y. Liu, F. Qian, et al., Bioresource Technol. 154 (2014) 209–214.
[57] R. Liu, X. He, M. Miao, S.i. Cao, X. Feng, J. Mater. Sci. Technol. 112 (2022) 202–211.
[58] X. Yu, H. Liu, Q. Wang, et al., ACS Sustain. Chem. Eng. 9 (2021) 13176–13187.
[59] H. Zhang, C. Lu, H. Hou, Y. Ma, S. Yuan, Chem. Eng. J. 370 (2019) 400–408.
[60] Z. Li, M. Wang, C. Jin, et al., Chem. Eng. J. 392 (2020) 123789.
[61] W. Jiang, J. Fang, Z. Fan, et al., J. Inorg. Chem. 26 (2011) 438–442.
[62] X. Zheng, X. Niu, D. Zhang, et al., Chem. Eng. J. 429 (2022) 132323.
[63] X. Wang, J. Jing, M. Zhou, R. Dewil, Chin. Chem. Lett. 34 (2023) 107621.
[64] Y. Li, R. Baghi, J. Filip, et al., ACS Sustain. Chem. Eng. 7 (2019) 8099–8108.
[65] Y. Li, H. Dong, J. Xiao, et al., J. Hazard. Mater. 442 (2023) 130014.
[66] X. Liu, Y. Pei, M. Cao, H. Yang, Y. Li, Chem. Eng. J. 450 (2022) 138194.
[67] X. Shu, H. Bi, J. Wang, et al., Environ. Sci. Pollut. Res. 29 (2022) 80399–80410.
[68] S. Oh, H. Nguyen, Environ. Res. 236 (2023) 116832.
[69] G. Jiao, H. Zhou, X. Li, J. Liu, D. She, Bioresource Technol. 384 (2023) 129357.
[70] Y. Tang, J. Kang, M. Wang, et al., J. Environ. Chem. Eng. 9 (2021) 105864.
[71] M. Wang, C. Jin, J. Kang, et al., Chem. Eng. J. 416 (2021) 128118.
[72] S. Gao, Z. Wang, H. Wang, et al., Appl. Surf. Sci. 599 (2022) 153917.
[73] L. He, H. Li, J. Wang, Q. Gao, X. Li, Environ. Sci. Pollut. Res. 29 (2022) 39249–39265.
[74] S. Pan, W. Jiang, L. Tian, et al., Sep. Purif. Technol. 312 (2023) 123452.
[75] J. Wu, H. Su, Z. Wang, et al., Sep. Purif. Technol. 297 (2022) 121487.
[76] W. Huang, X. Jin, Q. Li, et al., ACS Appl. Nano Mater. 6 (2023) 12497–12506.